文章编号： 1001-3806(2009)01-0046-04

基于弯曲损耗的光纤温度传感器

周广丽[1,2]，鄂书林[1*]，邓文渊[1]

(1. 中国科学院 长春光学精密机械与物理研究所 应用光学国家重点实验室，长春 130033；2. 中国科学院 研究生院，北京 100049)

摘要： 为了推导多模光纤弯曲损耗与弯曲半径、环境温度的关系，采用了 WKB 法求解非均匀直光纤的传播模数，并将弯曲光纤的有效折射率、弯曲光纤截止传播常数和光纤的热光效应同时引入到非均匀直光纤有效传播模数中。利用多模光纤进行实验验证，研制出测温灵敏度为 0.1/℃、测温范围为 10℃～70℃的光纤温度传感器。结果表明，弯曲损耗随弯曲半径的增大而减小，随环境温度的升高而减小，可以利用弯曲损耗测量环境温度。

关键词： 光纤光学；光纤温度传感器；WKB 法；有效折射率；截止传播常数；有效传播模数；弯曲损耗

中图分类号： TP212.14　　**文献标识码：** A

Optical fiber temperature sensors based on bending loss

ZHOU Guang-li[1,2], *E Shu-lin*[1], *DENG Wen-yuan*[1]

(1. Key Laboratory of Modern Applied Optics, Changchun Institute of Optics, Fine Mechanics and Physics, Chinese Academy of Sciences, Changchun 130033, China; 2. Graduate School, Chinese Academy of Sciences, Beijing 100049, China)

Abstract: In order to deduce that the bending loss was a function of curvature radius and temperature, WKB method was used to solve the number of modes of non-uniform straight fibers, the effective refractive index, the cut-off of propagation constant of bending fibers and thermo-optic effect of fibers were introduced to the number of modes of non-uniform straight fiber also. Choosing multimode graded-index optical fibers to get a temperature sensor, the sensitivity of the sensor was 0.1/℃ and the temperature sensing range was 10℃～70℃. The results indicate that the smaller the curvature radius and the temperature, the bigger the bending loss. Bending loss can be used to measure the temperature.

Key words: fiber optics; optical fiber temperature sensor; WKB method; effective refractive index; cut-off of propagation constant; effective number of modes; bending loss

引　言

光纤测温是上世纪 70 年代发展起来的一门新兴测温技术，与传统的温度传感器相比具有很多优点：光波不产生电磁干扰，也不怕电磁干扰，易被各种光探测器件接收，可方便地进行光电或电光转换，易与高度发展的现代电子装置和计算机相匹配，光纤工作频率宽，动态范围大，是一种低损耗传输线，光纤本身不带电，体积小质量轻，易弯曲，抗辐射性能好，特别适合于易燃、易爆、空间受严格限制及强电磁干扰等恶劣环境下使用。现在对光纤温度传感器的研究主要有分布式光纤温度传感器[1-3]、光纤光栅温度传感器[4-8]、光纤荧光温度传感器[9-13]和干涉型光纤温度传感器[14-15]。

弯曲光纤中光的传播受外界因素的调制，这个性质可以用来测量外界的干扰（温度、压力、震动等）。多模光纤弯曲时光纤内的有效传播模数减少产生弯曲损耗。当环境温度升高时，材料的折射率发生变化使多模弯曲光纤内的有效传播模式增多，输出光强增大，弯曲损耗降低。作者根据输出光强的变化监测环境温度的变化。基于弯曲损耗的光纤温度传感器具有动态的测温范围和高测温灵敏度，具有很广泛的应用前景。

1　理论研究

1.1　弯曲光纤的有效折射率分布

利用保角变换法将弯曲光纤等效为折射率重新分布的直光纤。弯曲光纤的有效折射率为[16]：

$$n^2 = n_0^2[1 + 2r\cos\theta/R] \tag{1}$$

式中，n 为有效折射率，n_0 为原直光纤的折射率，R，r，θ，a 如图 1 所示。

将 n 在 $0 \leqslant \theta \leqslant 2\pi$ 区间内求平均，可得有效折射率的平均值：

$$n(R) = \frac{2n_0}{\pi}\sqrt{1+\xi}\,\mathrm{E}\left[\frac{2\xi}{1+\xi}\right] \tag{2}$$

式中，$\xi = 2r/R$，$\mathrm{E}\left[\frac{2\xi}{1+\xi}\right]$是第 2 类完全椭圆积分，其表达式为：$\mathrm{E}\left[\frac{2\xi}{1+\xi}\right] = \int_0^1 (1-t^2)^{-1/2}\left(1 - \frac{2\xi}{1+\xi}t^2\right)^{1/2}\mathrm{d}t$。

作者简介：周广丽（1983-），女，硕士研究生，主要研究方向为光纤传感器。

* 通讯联系人。E-mail：eshulin@sohu.com

收稿日期：2007-11-21；收到修改稿日期：2008-01-23

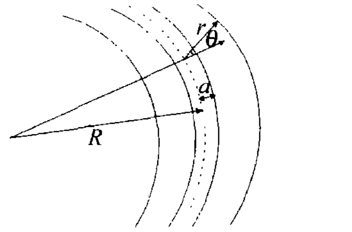

Fig. 1　The structure of bending optical fiber

1.2　弯曲光纤的有效传播模数和弯曲损耗

由 WKB 法解非均匀直光纤的标量波动方程得传播常数在 β_{min} 和 β_{max} 之间的模的总数为 $\nu(\beta)$[17]：

$$\nu(\beta) = \int_0^a [k^2n^2(r) - \beta^2]r\mathrm{d}r \qquad (3)$$

式中，k 为波数。渐变型光纤折射率分布可表示为：

$$n^2(r) = \begin{cases} n_1^2\left[1 - 2\Delta\left(\dfrac{r}{a}\right)^g\right], (0 \leqslant r \leqslant a) \\ n_1^2[1 - 2\Delta] = n_2^2, (r > a) \end{cases} \qquad (4)$$

式中，n_1，n_2 分别为纤芯和包层的折射率，a 见图 1，g 为光纤折射率分布系数，$\Delta = \dfrac{n_1^2 - n_2^2}{2n_1^2}$。

将(4)式代入(3)式积分得：

$$\nu(\beta) = \frac{1}{2}(k^2n_1^2 - \beta^2)a^2 - \frac{k^2a^2{d_{NA}}^2}{g+2} \qquad (5)$$

式中，d_{NA} 为数值孔径。令 $\beta = \beta_{min} = kn_2$，则直光纤中总的传播模数 N 为：

$$N = \frac{g}{2(g+2)}k^2a^2{d_{NA}}^2 \qquad (6)$$

弯曲光纤中每个传输模式(传播常数为 β)的损耗系数可以表示为[18]：

$$2\alpha = A\exp\left\{-\frac{2}{3}n_2kR\left(\frac{\beta^2 - n_2^2k^2}{n_2^2k^2} - \frac{2a}{R}\right)^{3/2}\right\} \qquad (7)$$

系数 A 对于不同类型的光纤有所不同，但在指数函数中，它的数值并不重要。对于任一个给定的曲率半径，存在着一个 $\beta = \beta_c$ 使指数函数的指数幂等于 −1。这个 β 的有效截止值为：

$$\beta_c = n_2k\left[1 + \frac{2a}{R} + \left(\frac{3}{2n_2kR}\right)^{2/3}\right]^{1/2} \qquad (8)$$

当 $R = \infty$ 时，$\beta_c = n_2k$，此为直光纤的正确截止值。

能在弯曲光纤中传播的模的总数小于直光纤中的模的总数，将(2)式、(8)式代入(5)式略去幂指数项得：

$$N_{eff}(R) = \bar{N}\left[1 - \frac{g+2}{g}\frac{2a{\bar{n}_2}^2}{R{d_{NA}}^2(R)}\right] \qquad (9)$$

其中，

$$\begin{cases} \bar{N} = \dfrac{g}{2(g+2)}k^2a^2{d_{NA}}^2(R) \\ {d_{NA}}^2(R) = {\bar{n}_1}^2 - {\bar{n}_2}^2 \end{cases} \qquad (10)$$

每个模式传输的光纤能量近似相等，则光纤的弯曲损耗可近似为：

$$\alpha(R,T) = 10\lg\left[\frac{P(R,T)}{P_0}\right] = 10\lg\left[\frac{N_{eff}(R,T)}{N(T_0)}\right] \qquad (11)$$

式中，T 和 P 表温度和功率，T_0 和 P_0 初始温度和功率。当外界温度发生变化，纤芯和包层材料的浓度随之发生变化，进而改变光纤的折射率。光纤折射率随温度的变化可表示为[19]：

$$\begin{cases} n_1(T) = n_1(T_0) + \displaystyle\int_{T_0}^{T}\frac{\mathrm{d}n_1}{\mathrm{d}T}\mathrm{d}T \\ n_2(T) = n_2(T_0) + \displaystyle\int_{T_0}^{T}\frac{\mathrm{d}n_2}{\mathrm{d}T}\mathrm{d}T \end{cases} \qquad (12)$$

式中，$K_1 = \dfrac{\mathrm{d}n_1}{\mathrm{d}T}$，$K_2 = \dfrac{\mathrm{d}n_2}{\mathrm{d}T}$ 分别为纤芯和包层材料的热光系数，用来量度折射率随温度的变化。

根据(12)式可以将弯曲光纤纤芯和包层材料的折射率与温度 T 的关系表示为：

$$\begin{cases} \bar{n}_1(R,T) = \bar{n}_1(R,T_0) + K_1(T - T_0) \\ \bar{n}_2(R,T) = \bar{n}_2(R,T_0) + K_2(T - T_0) \end{cases} \qquad (13)$$

将(6)式、(9)式、(10)式、(13)式，代入(11)式略去 K_1，K_2 的高次项，整理得温度为 T 时光纤的弯曲损耗：

$$\alpha(R,T) = 10\lg\left\{\frac{{\bar{n}_1}^2(T_0) - \delta{\bar{n}_2}^2(T_0) + 2(T - T_0)[K_1\bar{n}_1(T_0) - K_2\delta\bar{n}_2(T_0)]}{{n_1}^2(T_0) - {n_2}^2(T_0)}\right\} \qquad (14)$$

式中，

$$\delta = 1 + \frac{g+2}{g}\frac{2a}{R} \qquad (15)$$

以多模渐变型光纤(GIMM62.5/125μm，$g = 2$，数值孔

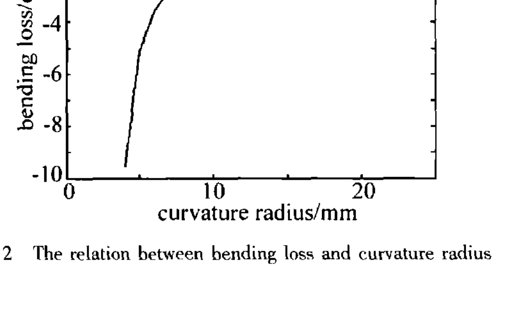

Fig. 2　The relation between bending loss and curvature radius

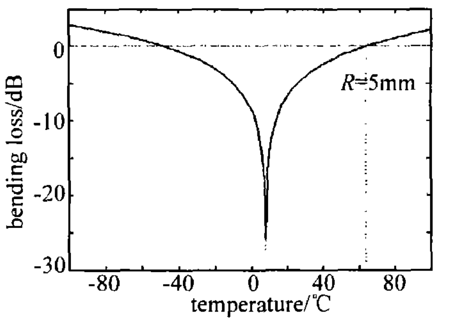

Fig. 3　The relation between bending loss and temperature

值径 $d_{NA} = 0.268$，$n_1 = 1.491$)为例，根据(14)式的理论推导得到弯曲损耗与弯曲半径和环境温度的关系如图 2 和图 3 所示。从图中可以看出，弯曲损耗随弯曲

半径的增大而减小,随环境温度的升高而减小。

1.3 传感器的测温范围和测温灵敏度

当弯曲半径一定时($R=R_0$),存在临界温度 T_{c1} 使光纤弯曲时有效传播模数为 0,此时光不能在光纤中传播;存在临界温度 T_{c2},此时弯曲光纤的传播模数与温度为 T_0 时直光纤的传播模数相等($N_{eff}(R_0,T_{c2})=N(T_0)$),光在其中传输时没有弯曲损耗。根据上面的理论分析,由(6)式、(9)式、(10)式、(13)式,得到临界温度 T_{c1},T_{c2}的表达式:

$$\begin{cases} T_{c1} = T_0 + \dfrac{-Y \pm \sqrt{Y^2 - 4XZ_1}}{2X} \\ T_{c2} = T_0 + \dfrac{-Y \pm \sqrt{Y^2 - 4XZ_2}}{2X} \end{cases} \tag{16}$$

其中,

$$\begin{cases} X = K_1^2 - \delta K_2^2 \\ Y = 2[K_1\bar{n}_1(T_0) - \delta K_2\bar{n}_2(T_0)] \\ Z_1 = \bar{n}_1{}^2(T_0) - \delta\bar{n}_2{}^2(T_0) \\ Z_2 = \bar{n}_1{}^2(T_0) - \delta\bar{n}_2{}^2(T_0) - d_{NA}{}^2(T_0) \end{cases} \tag{17}$$

1.4 传感器的测温灵敏度

由(6)式、(9)式、(10)式、(13)式,推导出光纤温度传感器的测温灵敏度为:

$$S = \frac{1}{P_0}\frac{dP(R,T)}{dT} = \frac{1}{N(T_0)}\frac{d}{dT}[N_{eff}(R,T)] = \frac{2}{d_{NA}{}^2(T_0)}[K_1\bar{n}_1(R,T_0) - K_2\delta\bar{n}_2(R,T_0)] \tag{18}$$

由(18)式可知,传感器的灵敏度与光纤参量和弯曲半径有关。选择数值孔径大、纤芯半径大、光纤材料的热光吸收系数大的多模光纤,能够提高该光纤传感器的测温灵敏度。

2 实验测量

作者选用多模渐变型光纤(GIMM62.5/125μm)研制光纤温度传感器。在室温 20℃、入射波长 $\lambda=1550$nm 时,该光纤的数值孔径为 $d_{NA}=0.268$,纤芯和包层的折射率分别为 $n_1=1.491$,$n_2=1.467$。纤芯和包层的热光系数分别为 $K_1=1.7744\times10^5$/℃,$K_2=-4.15\times10^{-4}$/℃。

实验装置如图 4 所示,光纤紧密缠绕在圆柱棒上,用真空干燥箱(DZF-6050)控制弯曲光纤周围的温度,光纤一头与可调谐激光器(Santac,TSL-210)连接,另一头与光功率计(Newport 1830-c)连接。

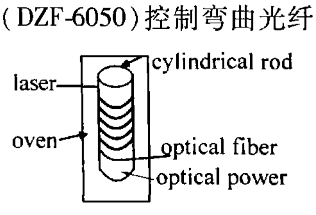

Fig.4 The experimental setup

当弯曲半径、缠绕圈数相同且入射光 $P_{in}=1$mW,$\lambda=1550$nm 时,得到输出光强与环境温度的关系如图 5 所示。

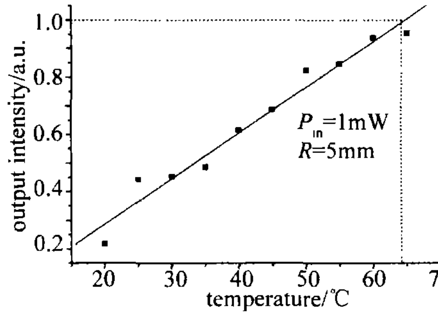

Fig.5 The relation between output intensity and temperature

可以得到以下结论:存在临界温度 $T_{c1}=10$℃,$T_{c2}=70$℃,温度在 T_{c1}和 T_{c2}之间时,输出光强随温度的升高而线性增强;当温度低于 10℃时,输出光强可忽略不计;当温度高于 70℃时,输出光强接近于输入光强,弯曲损耗为 0;该传感器的测温范围为 10℃~70℃,测温灵敏度为 0.1/℃。

当环境温度、缠绕圈数相同且入射光 $P_{in}=1$mW,$\lambda=1550$mm 时,得到输出光强与弯曲半径的关系如图 6 所示。

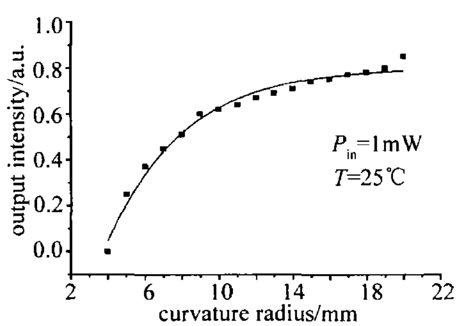

Fig.6 The relation between output intensity and curvature radius

可以得到以下结论:存在临届弯曲半径 $R_c=4$mm;当弯曲半径小于 4mm 时,输出光强为 0;当弯曲半径大于 4mm 时,输出光强随弯曲半径的增大而增强。

实验结论和理论推导基本相符。

3 结 论

利用 WKB 法研究了光纤中光的传播特性与弯曲半径和环境温度的关系,设计了基于弯曲损耗的光纤温度传感器,并选用多模渐变型光纤进行测量,得到了弯曲损耗与弯曲半径和环境温度的关系,与理论设计验证相符。

参 考 文 献

[1] ROGERS A J. Distributed optical-fiber sensors for the measurement of pressure, strain and temperature [J]. Physics Report, 1988, 169(2):

118-119.

[2] GUNES Y, SAIT E K. A distributed optical fiber sensor for temperature detection in power cables [J]. Sensors and Actuators, 2006, A125 (2): 148-155.

[3] ZHANG Y, ZHANG Z X, KIM I S. Design and implementation of long range distributed optical fiber temperature sensor system [J]. Opto-electronic Engineering, 2005, 32(4): 45-48 (in Chinese).

[4] MOREY W W, MELTZ G, GLENN W H. Fiber optic Bragg grating sensors [J]. SPIE, 1989, 1169: 98-107.

[5] ALLSOP T, FLOREANI F, WEBB D J, *et al*. The bending and temperature characteristics of long period gratings written in elliptical core step-index fibre [J]. SPIE, 2005, 5855: 711-714.

[6] IADICICCO A, CAMPOPIANO S, CUTOLO A, *et al*. Simultaneous measurements of refractive index and temperature by non-uniform thinned fiber Bragg gratings [J]. SPIE, 2005, 5855: 479-482.

[7] ZHAN Y G, CAI H W, XIANG Sh Q, *et al*. Study on high resolution fiber Bragg grating temperature sensor [J]. Chinese Journal of Lasers, 2005, 32(1): 83-86 (in Chinese).

[8] ZHOU Zh, WANG H Zh, OU J P. Fiber Bragg grating packaged temperature sensor without exterior load affection [J]. Transducer and Microsystem Technology, 2006, 25(3): 57-60 (in Chinese).

[9] TAO Sh Q, JAYAPRAKASH A. A fiber optic temperature sensor with an epoxy-glue membrane as a temperature indicator [J]. Sensors and Actuators, 2006, B119(2): 615-620.

[10] AIZAWA H, KATSUMATA T, KOMUROA S, *et al*. Fluorescence thermometer based on the photoluminescence intensity ratio in Tb doped phosphor materials [J]. Sensors and Actuators, 2006, A126 (1): 78-82.

[11] BAEK S G, JEONG Y C, NILSSON J, *et al*. Temperature-dependent fluorescence characteristics of an ytterbium-sensitized erbium-doped silica fiber for sensor applications [J]. Optical Fiber Technology, 2006, 12(1): 10-19.

[12] ZHAO Y, RONG M, WANG Y, *et al*. Fiber-optic temperature sensors based on semiconductor optical absorption [J]. Journal of Optoelectronics · Laser, 2003, 14(2): 140-142 (in Chinese).

[13] WU J L, WANG Y T, GUO Y. Ruby fluorescence wavelength—division fiber-optic temperature sensors [J]. Journal of Optoelectronics · Laser, 2006, 17(4): 427-429 (in Chinese).

[14] ABI KAED BEY S K, SUN T, GRATTAN K T V. Optimization of a long-period grating-based Mach-Zehnder interferometer for temperature measurement [J]. Opt Commun, 2007, 272(1): 15-21.

[15] BI W H, WANG X, LANG L Y. The optical fiber F-P interferometric temperature measurement [J]. Journal of Optoelectronics · Laser, 2002, 13(12): 1316-1317 (in Chinese).

[16] WANG X Zh, BIAN B M, JI Y J, *et al*. Theoretical model modify of bending loss of mono-mode fiber [J]. Scope on Acta Photonica Sinica, 2006, 35(6): 819-823 (in Chinese).

[17] OKOSHI T, LIU Sh H, LIANG J M. Optical fiber communication [M]. Beijing: Posts & Telecom Press, 1989: 125 (in Chinese).

[18] MILLER S E, CHYNOWETH A G, ZHANG B Q. Optical fiber telecommunication [M]. Beijing: Posts & Telecom Press, 1983: 65 (in Chinese).

[19] MARKIJAN B. Optical fiber sensor for temperature measuring [C]//The Third ICIM/ECSSM'96. Lyon, France: Elsevier, 1996: 198-202.

(上接第45页)

[14] Buddy Products, Inc. Laser buddy's business wire [EB/OL]. (2007-01-02) [2007-05-13]. http://www.laserbuddy.com/business/company/dex.htm.

[15] DAWSON M. Imaging using LEDs and lasers [J/OL]. (2005-11-10) [2007-05-14]. http://phys.strath.ac.uk/12-150/MDsum12.htm.

[16] XU S H. Development of "optics valley" and optoelectronic [EB/OL]. (2001-03-02) [2007-05-14]. http://www.bjx.com.cn/files/wx/sjdzyqj/2001-6/19.htm (in Chinese).

[17] Photonics Inc. 447nm blue laser products [EB/OL]. (2005-10-13) [2007-05-14]. http://www.photonics.com/directory/XQ/ASP/profilepage.t72750000/QX/viewcop2.htm.

[18] Sun Instruments Inc. 447nm blue laser products introduction [EB/OL]. (2006-01-23) [2007-05-15]. http://www.sun-ins.com/Litecyclesproduct.htm.

[19] OGILVY H, WITHFORD M J, PIPER J A. Intracavity second and third harmonic generation at 671nm and 447nm from a *Q*-switched Nd:$GdVO_4$ laser [R]. Chiba, Japan: Theoptical Society of Japan, 2005: 1400-1430.

[20] HE J L, HU X P, ZHU S N, *et al*. Efficient generation of red and blue light in a dual-structure periodically poled $LiTaO_3$ crystal [J]. Chinese Physics Letter, 2003, 20(12): 2175-2177.

[21] MA Y, PENG X C. Red and blue light generations in a periodically poled $LiTaO_3$ by 1342nm laser [J]. Chinese Journal of Lasers, 2005, 32(2): 262-264 (in Chinese).

[22] OU T H. Optimization of intracavity frequency-tripled all solid-state laser system: 355nm and 447nm [M]. Taipei: National Chiao Tung University, 2005: 223-227 (in Chinese).

[23] CHEN Y F, CHEN Y S, OU T H. Compact efficient diode-pumped Nd:YVO_4 *Q*-switched blue laser with intracavity frequency tripling [J]. Appl Phys, 2005, B81(4): 517-520.

[24] LI J. All-solid-state continuous wave intracavity frequency-tripled Nd:YVO_4-LiB_3O_4 blue laser using double-resonant approach [J]. Opt Commun, 2007, 277(1): 114-117.

[25] Cernic Cernet. The critical technologies of all-solid-state blue and green lasers were solved by institute of research on the structure of matter in Chinese academy of sciences. [EB/OL]. (2007-03-15) [2007-05-20]. http://www.edu.cn/cheng_guo_zhan_shi_1085/20070327/t20070327-224992.shtml (in Chinese).